

Experimental Study of Plastic Wave Velocity in Snow

By

Atsushi Sato*

*Shinjo Branch, National Research Center for Disaster Prevention
Tokamachi, Shinjo, Yamagata, 996, Japan*

Abstract

A plastic wave is generated at the head of a body moving in snow at high speed. The propagation of these waves in dry snow was studied in order to evaluate the effect of impact velocity and snow density on the velocity of the wave. Laboratory experiments were carried out by impacting snow at various speeds from 4 m/s to 49 m/s. The range of snow density used in the experiments was from 0.15 Mg/m³ to 0.54 Mg/m³.

The plastic wave speed U was obtained as a function of initial snow density and impact velocity v . The ratio of U to v increased sharply as the density increased, and also increased as v decreased.

The terminal plastic velocity V^* was estimated as the maximum velocity of plastic wave existing in snow, and the critical plastic velocity V^{**} was calculated from the snow density increase to the ice density at the wave front. It was shown that these two velocities are almost equal to the elastic wave velocity of the snow.

1. Introduction

Compared with the numerous works on low speed compression tests on snow, there are few reports on high speed compression studies, including shock waves in snow.

The first attempt to measure the plastic shock wave was made by Napadensky (1964). She explosively compressed high density snow samples of polar firm in Greenland. Yosida (1974) suggested that snow may exert a large resistance to a moving body which impacts snow at the speed of a plastic wave. Sato and Wakahama (1976) studied plastic wave propagation at low impact velocities. Gubler (1977) made explosion tests in the field. Sato and Brown (1983) measured the wave attenuation in wet snow using an electromagnetic stress-wave generator. Although theoretical work was done by Brown (1980, 1983), there have been few experimental and theoretical studies on plastic wave velocity.

*Second Snow Disaster Prevention Laboratory, Shinjo Branch

As snow shows very complicated mechanical behavior, plastic wave propagation has to be influenced by many factors such as impact velocity, snow density, water content, snow temperature and so on. In this paper, we focus on the measurement of the plastic wave velocity as a function of impact velocity and density. Also observed are the plastic wave propagation with high speed photographs and thin sections of snow specimens to investigate the density change due to the plastic wave.

2. Experimental procedure

(a) Apparatus for compression

A wide range of impact velocities was obtained by using the 4 different apparatus described below. Thus the impact velocities ranged from 4 m/s to 49 m/s.

First a cylindrical metal weight with a diameter and thickness of 50 mm was dropped from a height of 2 m. This is shown in Figure 1 with the two measuring methods of wave velocity described below. By this apparatus, impact speed of 4 to 5 m/s was obtained. Second, a spring gun was designed to eject an aluminum disk of 50 mm diameter and 30 mm thickness to compress the snow specimen. This apparatus is shown in Figure 2. The impact speed varied from 5 to 11 m/s.

The third was the Hopkinson bar method, a schematic figure of which is shown in Figure 3. Using nitrogen gas with 6 bars of pressure, an aluminum bar of 30 mm in diameter was accelerated in a 2 m launch tube. The snow specimen placed on the end of the tube was compressed at a speed of 20 to 25 m/s. For the fourth method a pitching machine was used, which had a rotating arm driven by three strong springs to pitch a baseball. This can be seen in Photo 1. In our experiment, a high speed ball hit a small

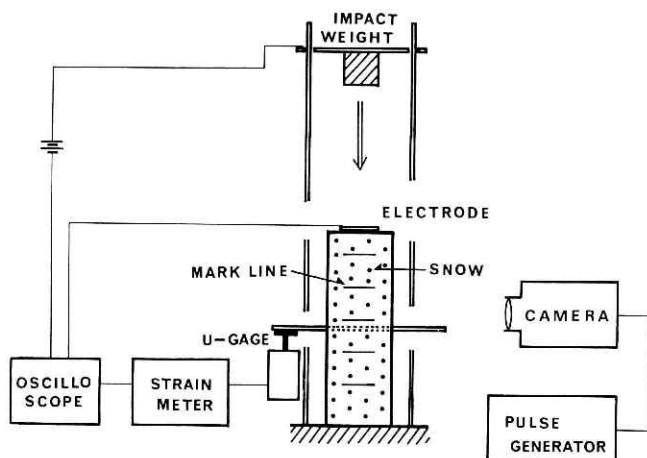


Fig. 1 A metalweight dropping method with two plastic wave velocity measuring method, a high speed photography and a pressure transducer.

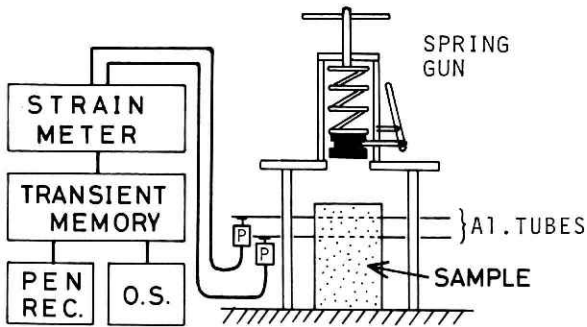


Fig. 2 A measuring system of plastic wave velocity, using pressure transducers(p) set up with the spring gun.

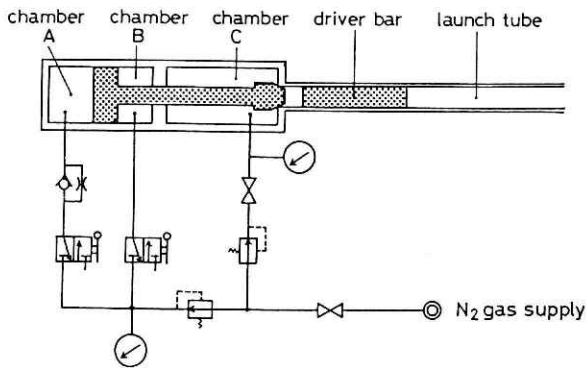


Fig. 3 Hopkinson pressure bar method. A 6 bar nitrogen gas was used to eject a driver bar.

wooden plate on the surface of snow specimen to generate a plane plastic wave. The impact speed generated by this device ranged from 24 to 49 m/s. Table 1 summarizes the described apparatus with driving force, impact direction, and gained impact velocity.

(b) Methods of measuring the plastic wave velocity

The compressive speed was measured in all tests. Two split parallel laser beams were set on the sample surface to detect the impactor speed just before the impact, as

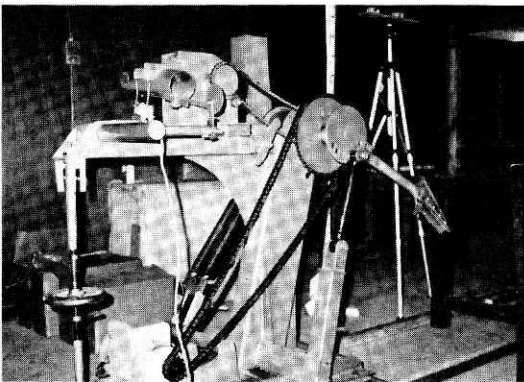


Photo 1 A pitching machine, which generated impact speed from 24 to 49 m/s.

Table 1 Apparatus for plastic wave generation

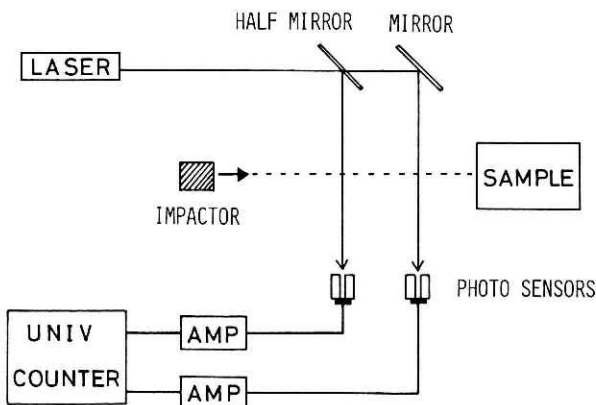
APPARATUS	DRIVING FORCE	IMPACT DIRECTION	VELOCITY
METAL WEIGHT DROPPING METHOD	GRAVITY	VERTICAL	4-5 m/s (14-18 km/h)
SPRING METHOD	COIL SPRING	VERTICAL	5-10 (18-40)
HOPKINSON BAR METHOD	HIGH PRESSURE N ₂ GAS	HORIZONTAL	20-25 (72-90)
PITCHING MACHINE METHOD	SPRING & MOTOR	HORIZONTAL	24-49 (86-176)

described in Figure 4. Time intervals of cutting off the 2 beams by the impactor were measured by a universal counter. The measured impact velocity had a relative error of less than 1 %.

In order to observe the generation and propagation of the plastic wave, high speed photographs using 16 mm film were used. Two different cameras were used according to the wave speed (HYCAM with a maximum film speed of 4,500 fps and DYNAFAX-350 with a maximum speed of 35,000 fps).

The front surface of the snow specimen was lined beforehand at 10 mm intervals by carbon powder in 2 mm widths. By analyzing the high speed photos, time-travel curves were obtained, as shown in Figure 5. This graph gives impact velocity, plastic wave velocity, and particle velocity.

Small pressure transducers were also used to detect the plastic wave speed, as shown in Figure 2. A plastic wave front which is accompanied by a pressure jump hit successively two light aluminum tubes buried in the snow. Plastic wave velocity was calculated by the intervening space of the aluminum tubes and the time interval recorded with a transient memory.

**Fig. 4** A schematic diagram of an impact velocity measuring system.

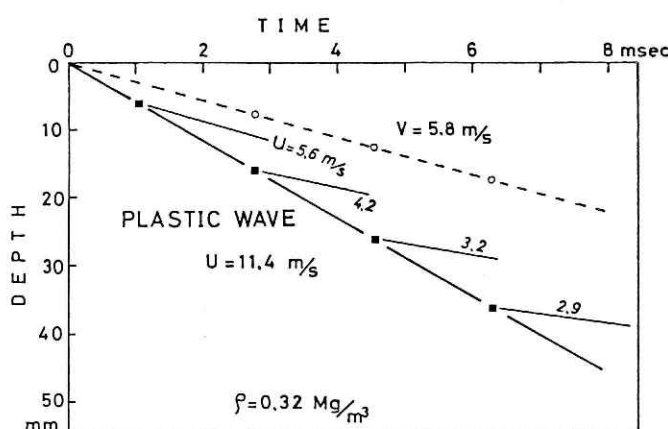


Fig. 5 An example of high speed photos analysis, gradients of thick line, thin lines, and dashed line give the velocities of plastic wave, particle, and impact respectively.

(c) Snow samples

Naturally deposited snow was taken from the field into a cold room and tested. Dry, freshly deposited snow and dry settled snow were used as samples. To avoid the influence of the layer structure of naturally deposited snow, samples were taken from a homogeneous layer, and compression was made always parallel to the boundary planes of the deposited layers. The experiments were conducted in a cold room of temperature around -6°C .

3. Experimental results

(a) The effect of impact velocity on plastic wave velocity

Plastic wave velocities U were plotted against the impact velocity v , as shown in Figure 6, and were divided into three groups of initial snow density. These groups are composed of "Shinsetsu" (freshly deposited snow), "Shimari Yuki" (settled snow), and "Kata-shimari Yuki" (compacted snow), the respective density ranges of which are $0.15 - 0.20 \text{ Mg/m}^3$, $0.20 - 0.30 \text{ Mg/m}^3$, and $0.30 - 0.54 \text{ Mg/m}^3$.

After plotting on a logarithmic graph, it was found that the data lie on a straight line for each group. Regression lines were calculated as a form of

$$U = av^b \quad (1)$$

Standard deviation for each group was calculated as 0.99 for (a), 0.98 for (b), and 0.97 for (c), as seen in Figure 6. A coefficient a and an index b can be thought of functions of density, and are listed in table 1 for these three groups.

(b) Particle velocity

As shown in Figure 5, particle velocities were calculated from the gradients of thin solid lines. These values decrease from $u = 5.6 \text{ m/s}$ to 2.9 m/s with an increase of depth in this case. For the three different snow densities, changes of particle velocities in

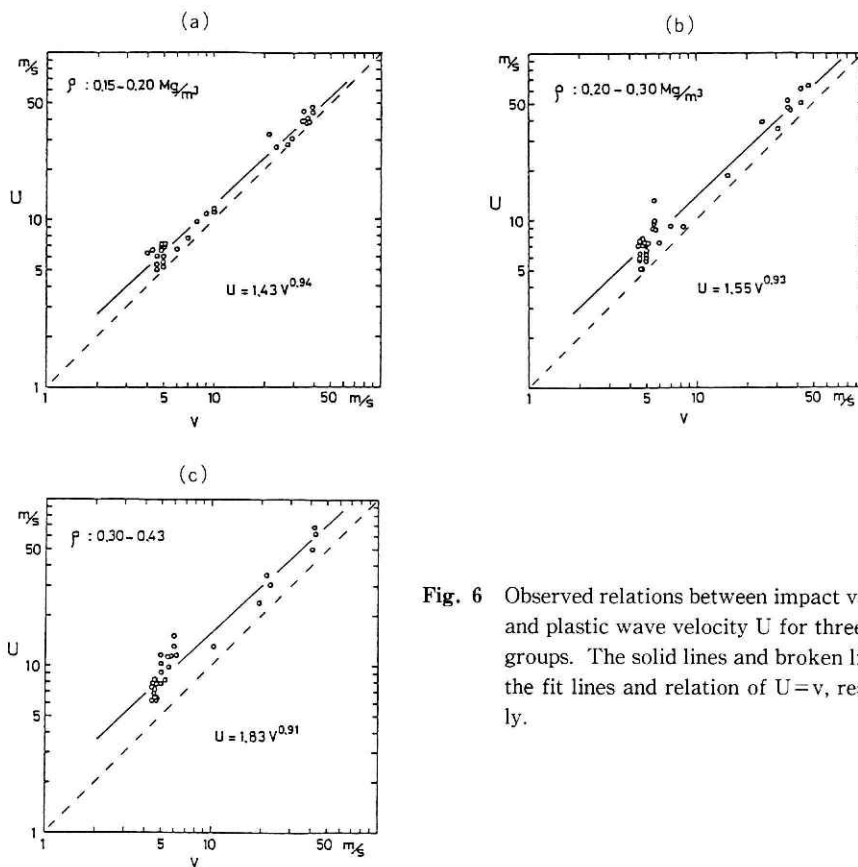


Fig. 6 Observed relations between impact velocity v and plastic wave velocity U for three density groups. The solid lines and broken line show the fit lines and relation of $U = v$, respectively.

relation to the depth from the impact surface are shown in Figure 7. Lower density snows very little decrease of particle velocity with depth, while higher density snow exhibits a significant decrease.

(c) Density increase

Thin section observations of snow specimens after impact, and structural changes of the snow were made, as reported in Wakahama & Sato (1977). Two zones were seen : a heavily compacted zone located just below the impactor, and a zone with unchanged structure in the forward portion. Density measurements were made in detail to investigate the changes in the compacted zone, as shown in Figure 8. The portion A represents the compacted zone and B, the undisturbed zone. Here, the density for portion B remained at 0.30 Mg/m^3 , which was the same as the original sample density. On the other hand, portion A showed a density jump from 0.30 to 0.49 Mg/m^3 at the boundary, and a gradual increase to 0.61 Mg/m^3 at the top of this portion.

4. Discussions

(a) Upper limit of plastic wave

We obtained an equation (1), which establishes a relation between impact velocity v

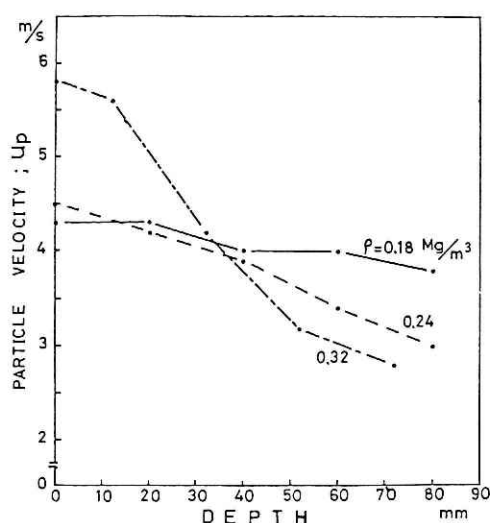


Fig. 7 Variation of particle velocity with depth.

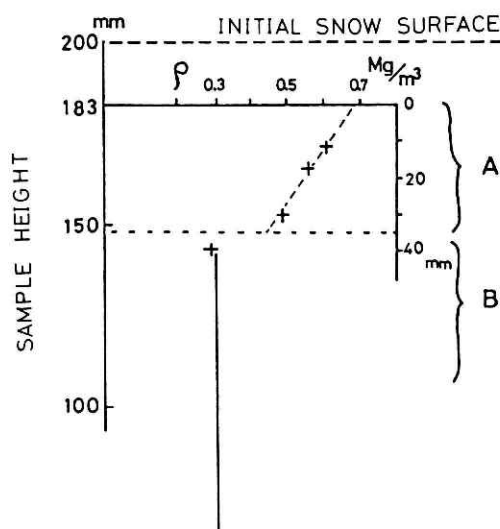


Fig. 8 Change of snow density along the impact direction. Impact started at 200mm and stopped at 183mm with respect to the height of the snow specimen.

and plastic wave velocity U . A coefficient a and an index b were investigated as functions of the initial snow density, as shown in Figure 9. Apparent relations were found to be

$$a = 2.25\rho_0 + 1.01 \quad (2)$$

$$b = -0.17\rho_0 + 0.97 \quad (3)$$

Then an empirical equation $U = av^b$ can be written as a parameter of snow density.

The obtained equation (1) is larger than the line $U = v$ for all experimental impact velocities. This means that the plastically deformed zone always advances faster than the impactor in the snow. In addition, the index b is smaller than the unity for all initial snow densities. Therefore the two lines, (1) and $U = v$, must intersect at some high impact velocity v , where the impact velocity is equal to the plastic wave velocity. We call this

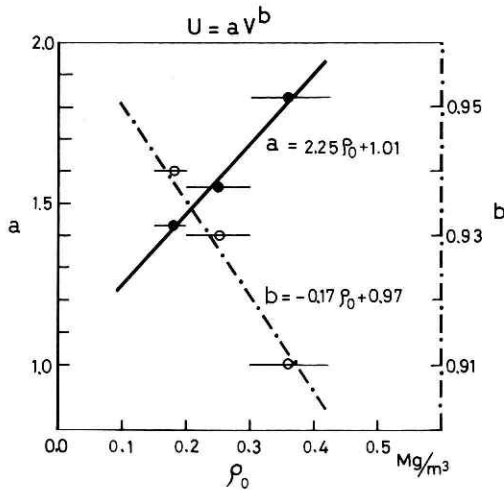


Fig. 9 Effect of initial snow density on coefficients a and indices b.

velocity the terminal plastic velocity, which expressed as

$$V^* = \exp \left[(\ln a) / (1 - b) \right] \tag{4}$$

We have listed the V^* values for the three density groups in Table 2.

Table 2 Calculated constants a, b, terminal plastic velocity V^* , critical plastic velocity V^{**} , and measured longitudinal elastic velocity V_E for the three density groups.

Density (Mg/m ³)	U = av ^b		V* (m/s)	V** (m/s)		V _E (Elastic) (m/s)
	a	b		Δ = 0.1	Δ = 0.2	
0.15–0.20 (0.18)	1.43	0.94	388	142	190	(200–350)
0.21–0.30 (0.25)	1.55	0.93	524	275	400	400–700
0.31–0.43 (0.35)	1.83	0.91	824	430	700	750–1200

V* : Intersection of $U = av^b$ and $U = v$
V** : Density jump to the $\rho_{ice} = 0.917 \text{ Mg/m}^3$

(b) Density increase

The plastic wave velocity can be argued from the conservation of mass. As seen in the previous section, the elastic wave is much faster than the plastic one in the range experimented. Therefore we can assume that effects of the elastic wave have died out by the time the plastic wave arrives at a particle.

It is convenient to use the impact velocity v rather than the particle velocity u_p since u_p is difficult to measure in the compression tests. As seen above, the particle velocity

u_p decreases from the initial velocity, which is equal to the impact velocity v , as the snow depth increases. The extent of this decrease differs depending on snow density. The ratio r of the particle velocity to the impact velocity is written as the following equation and shown in Figure 10,

$$r = u_p/v = \alpha + \beta \rho_0 + \gamma \rho_0^2 \quad (5)$$

In the following analysis, a depth of 30mm was used, so that the coefficients become $\alpha = 1.0$, $\beta = 0.19$, and $\gamma = -2.68$ (Sato 1980). Then the density behind the wave front was calculated and expressed as

$$\rho_1 = a \rho_0 / [(a - r v^{1-b})(1 + \Delta)] \quad (6)$$

where Δ is the ratio of diverged area, which is the lateral expanse behind the wave front as seen in Figure 11, and estimated as 0.1 to 0.2 (Sato, 1980). In other words Δ is a correlation factor which enables application of the law of mass conservation to this phenomena. Equation (6) is graphically expressed in Figure 12 for the cases of initial density $\rho_0 = 0.18 \text{ Mg/m}^3$ and 0.35 Mg/m^3 . The above eluation gives $= 0.52 \text{ Mg/m}^3$ for the case of $\rho_0 = 0.35$, $\Delta = 0.2$ and $v = 5 \text{ m/s}$, which agrees with the observed value shown in Figure 9. The equation (6) shows that ρ_1 reaches 0.6 Mg/m^3 at $v = 30 \text{ m/s}$ and 0.63 at $v = 50 \text{ m/s}$ for the same initial density $\rho_0 = 0.35 \text{ Mg/m}^3$.

The maximum density of ρ_1 could be the ice density $\rho_{ice} = 0.9917 \text{ Mg/m}^3$. For such a critical velocity to cause ρ_{ice} must be calculated by the equation (6). We call this the

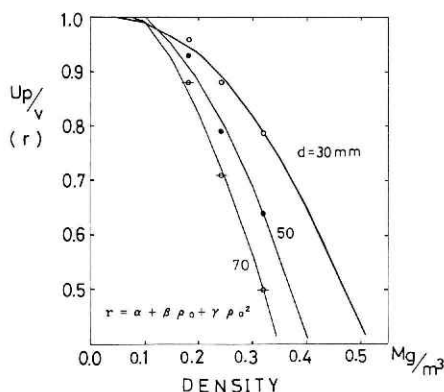
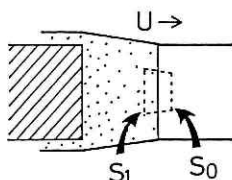


Fig. 10 Effect of density on the ratio of particle velocity to impact velocity. The depth from the impact surface is expressed by d .



$$\Delta = (S_1 - S_0) / S_0$$

Fig. 11 Lateral expanse of snow by passing the wave front. The ratio of the expanse is denoted as Δ .

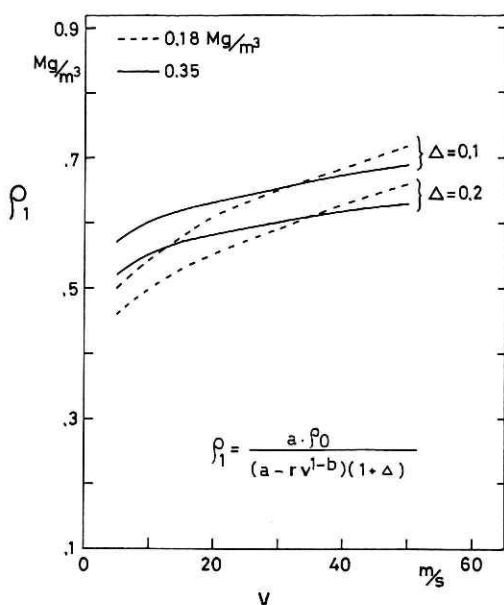


Fig. 12 Effect of impact velocity on the density change behind the wave front. The initial snow densities were 0.18 Mg/m^3 (dotted line) and 0.35 Mg/m^3 (solid line).

critical plastic velocity and it is denoted as V^{**} . The calculated velocities V^{**} are shown in Table 2 for the three initial density groups.

(c) Plastic wave velocity

Combining the conservation of mass and equation (6), the equation for plastic wave velocity is obtained as

$$U = arv / [a + (rv^{1-b} - a)(1 + \Delta)] \quad (7)$$

which is a function of the initial density and impact velocity and also has parameter of Δ .

From the equation (7) the ratio U/v is calculated as a function of density and impact velocity v . Calculated curves for these three different impact velocities are shown in Figure 13. Also plotted are experimental values classified into three groups of impact velocities. Experimental values have a lot of scatter, but there is a clear tendency for U/v to become higher for lower v , and also for U/v to increase with increasing initial density.

The obtained equation (7) shows the substantial agreement with the observed values, especially with respect to v dependence. Clearer dependence of U/v on v is shown in Figure 14 with the parameters of density. For lower density, only a small change is seen as v increases. However high density snow has a large value of U/v , and this decreases as v increases. This could be interpreted as time dependent viscoelasticity.

(d) Maximum velocity of the plastic wave

In the previous section the critical plastic velocity V^* was obtained as an equivalent velocity of the impact speed. These values are plotted in Figure 15 against the snow density, also expressed are the measured elastic wave velocities in snow (Yamada et al, 1974) which scatter in the dotted area. As seen in this figure, V^* agrees well with the elastic wave velocities. It is well known that if an object flies in the air at a higher speed

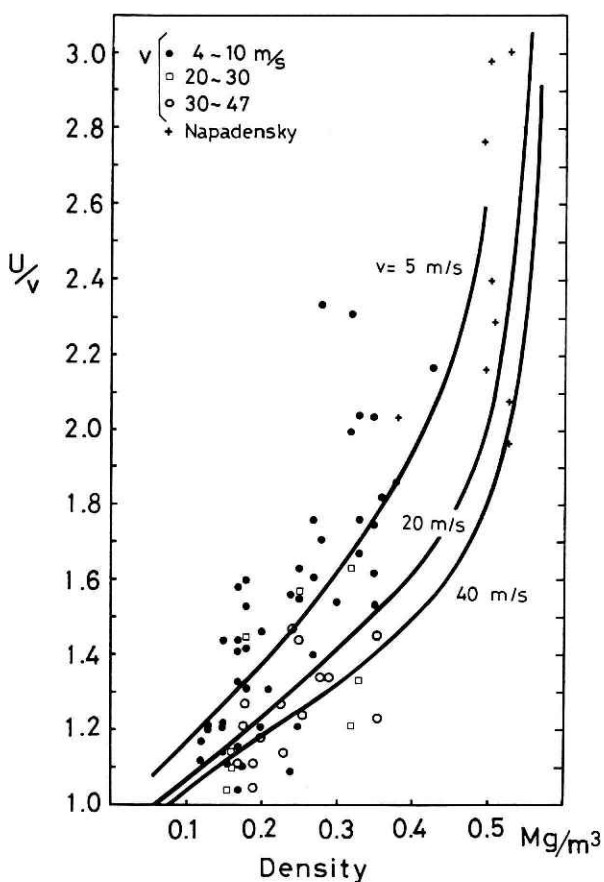


Fig. 13 Variation of U/v with density. Dots express the measured values and lines express calculations.

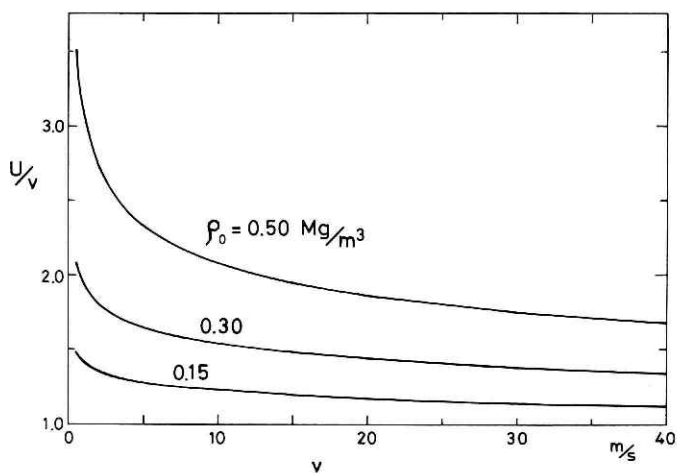


Fig. 14 Calculated variation of U/v with impact velocity v .

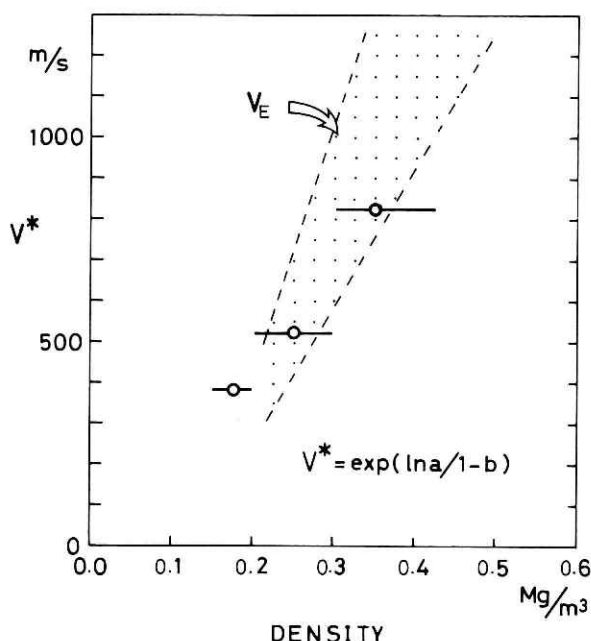


Fig. 15 Variation of terminal plastic velocity V^* with density, and observed longitudinal elastic wave velocity V_E .

than sound, a shock wave is generated in the air. Even for the propagation of sound in snow, there could be the interaction between the ice framework and void air (Sommerfeld, 1981). If an impactor moves with a velocity higher than the sonic velocity, there might appear a new shock wave in snow, and a strong interaction with the ice framework.

From the other viewpoint of density increase at the plastic wave front, the critical plastic velocity V^{**} , which causes the density increase of snow to that of the ice, is calculated and listed in Table 2. As seen here, these values of V^{**} are about the same range of sonic velocity.

It can be inferred that there exist normal plastic waves when the impact velocities are smaller than V^* or V^{**} , and that, at these impact velocities, a plastic wave is caught by the impactor and the snow is compressed to the ice density at the wave front.

5. Conclusion

A relation between impact velocity and plastic wave velocity was obtained empirically for a wide range of both dry snow density and impact velocity. Measurements showed that the snow particle velocity decreases with the distance ahead of the impactor, and is dependent on the initial snow density even if the distance from the impactor is the same.

The conservation of mass was introduced to estimate the density increase at the wave front, and plastic wave velocity as a function of initial snow density. These results

agree with those observed. Next it was shown that the ratio of plastic wave velocity to impact wave velocity increases sharply with increasing density, and decreases with increasing impact velocity.

Finally it was shown that two critical impact velocities can be estimated from the intersection of lines $U=v$ and $U=av^b$, and from calculations which assume that density increases to the ice density at the plastic wave front, and these are close to the velocity of longitudinal elastic waves in snow as a function of density.

6. Acknowledgment

The author wishes to express his gratitude for the kind guidance and encouragement received from professor G. Wakahama of the Institute of Low Temperature Science, Hokkaido University, Sapporo. He is also indebted to Professors S. Kinoshita and Y. Suzuki of the same institute for their helpful discussions, and Prof. R. L. Brown of Montana State University and Dr. D. M. McClung of NRC Canada for their critical readings of the manuscript. Acknowledgment is also due to Dr. T. Nakamura and Dr. M. Higashiura of Shinjo Branch, National Research Center for Disaster Prevention, for their encouragement of the Publication.

References

- 1) Brown, R.L. (1980) Propagation of stress waves in alpine snow. *Journal of Glaciology*, **26**(94), 235-243.
- 2) Brown, R.L. (1983) A comparison of unsteady wave propagation for various snowpack properties. *Annals of Glaciology*, **4**, International Glaciological Society, 30-36.
- 3) Gubler, H. (1977) Artificial release of avalanches by explosives. *Journal of Glaciology*, **19**(81), 419-429.
- 4) Napadensky, H. (1964) Dynamic response of snow to high rates of loading. *CRREL Research Report*, 119.
- 5) Sato, A. & Wakahama, G. (1976) Plastic wave in snow. *Low Temperature Science*, Ser.A, **34**, 59-69.
- 6) Sato, A. (1980) A study of high speed plastic compression of snow. PhD thesis, Hokkaido University, Sapporo.
- 7) Sato, A. & Brown, R.L. (1983) An evaluation of hock waves in unsaturated wet snow. *Annals of Glaciology* 4, International Glaciological Society, 241-245.
- 8) Sommerfeld, R.A. (1981) A review of snow acoustics. *Proceedins of a Workshop on the Properties of snow*, Snowbird, Utah, 62-66.
- 9) Wakahama, G & Sato A. (1977) Propagation of a plastic wave in snow. *Journal of Glaciology*, **19**(81), 175-183.
- 10) Yamada, T., Hasemi, T., Izumi, K., & Sato, A. (1974) On the dependencies of the velocities of P- and S-waves and thermal conductivity of snow upon the texture of snow. *Low Temperature Science*, Ser. A, **32**, 71-80.
- 11) Yosida, Z. (1974) Theoretical studies on snow removal by a plough. I & II. *Low Temperature Science*, Ser. A, **32**, 39-70.

(Manuscript Received January 6, 1987)

積雪の塑性波速度の実験的研究

佐藤篤司*

国立防災科学技術センター新庄支所

要 旨

積雪の高速変形現象,特にこれに付随する塑性波は最近注目を集めているテーマである。雪崩のおよぼす巨大な衝撃力や高速除雪において発生する抵抗力を考える際に基本的に重要であることが指摘されているからである。

本報告は圧縮速度と積雪密度が乾雪の塑性波速度におよぼす影響を実験的に調べたものである。試験に用いられた衝撃速度は4 m/sから49 m/sで、積雪密度は0.15 Mg/m³から0.54 Mg/m³の各範囲である。

塑性波速度 U は積雪の初期密度および衝撃速度 v の関数として求め、比 U/v は初期密度の増加と共に急激に増大し、また v の増加に対して減少することが明らかになった。

塑性波速度の上限として終端速度 V^* が演えきのに求められた。また波面で積雪が圧密を受け水の密度になるときの臨界速度 V^{**} が計算された。さらにこれは両速度が実験的に録めた積雪の縦波弾性波速度にほぼ等しいことが示された。

*雪害防災第2研究室